Molecular dynamics study on the evaporation part of the kinetic boundary condition at the interface between water and water vapor

Tatsuya Ishiyama*, Takeru Yano* and Shigeo Fujikawa*

*Division of Mechanical Science, Hokkaido University, Sapporo 060-8628, Japan

Abstract. Molecular dynamics simulations of vapor–liquid equilibrium states and those of evaporation from liquid phase into a virtual vacuum are performed for water. In spite of the formation of molecular clusters in the vapor phase and the presence of the preferential orientation of molecules at the interface due to uneven sharing of the bonding electron pair, essentially the same results as in our previous study for argon are obtained. That is, when the bulk liquid temperature is relatively low, the distribution function of evaporation can be expressed as the product of the equilibrium distribution of saturated vapor at the temperature in the bulk liquid phase and a well-defined evaporation coefficient, which is determined as a decreasing function of the liquid temperature, and is found to approach unity with the decrease of the temperature.

INTRODUCTION

The kinetic boundary condition at an interface between a vapor and its condensed phase

$$f_{\text{out}} = \alpha f^{\text{e}} + (1-\alpha) f^{\text{r}} \quad (\xi_z > 0), \tag{1}$$

has widely been used so far, where f_{out} is the distribution function of outgoing molecules from the interface, α is a parameter between zero and unity, sometimes called the condensation coefficient, f^{e} is the equilibrium distribution of saturated vapor at the temperature of the condensed phase, f^{r} is, usually, the distribution function of the diffuse reflection at the temperature, and ξ_z is the velocity component normal to the interface (for simplicity, we consider a planar interface at rest, facing the positive z direction). We call αf^{e} the evaporation part and $(1-\alpha) f^{\text{r}}$ the reflection part.

Many important phenomena associated with evaporation and condensation at the interface have been clarified by the use of this type of kinetic boundary condition (see [1, 2, 3] and references therein). However, its physical validity still remains to be established, and the related studies on the basis of the molecular dynamics (MD) method have just been started [4, 5, 6, 7]. In a previous paper [7], to study the kinetic boundary condition at an interface between argon vapor and its condensed phase, we have carried out MD simulations of vapor–liquid (or solid) equilibrium states (see Fig. 1) and those of evaporation from the liquid (or solid) phase into a virtual vacuum. As the result, we have shown that, in the case that the temperature of the bulk condensed phase T_ℓ is near the triple point temperature of argon, the distribution function for molecules evaporating into vacuum is given by $\alpha_e \rho_v \hat{f}^*$, where ρ_v is the saturated vapor density, $\rho_v \hat{f}^*$ is the half-Maxwellian of saturated vapor

$$\rho_v \hat{f}^* = \frac{\rho_v}{(2\pi R T_\ell)^{3/2}} \exp\Big(- \frac{\xi_x^2 + \xi_y^2 + \xi_z^2}{2RT_\ell} \Big) \quad (\xi_z > 0), \tag{2}$$

(R is the gas constant and ξ_x and ξ_y are the velocity components tangential to the interface), and α_e is the evaporation coefficient defined by the ratio of an averaged mass flux evaporating into vacuum $\langle J_{\text{evap}} \rangle$ to averaged outgoing mass flux in the equilibrium state $\langle J_{\text{out}} \rangle_{\text{eq}}$,

$$\alpha_e = \frac{\langle J_{\text{evap}} \rangle}{\langle J_{\text{out}} \rangle_{\text{eq}}}, \tag{3}$$

where the brackets denote the ensemble average (see Fig. 2).

CP762, *Rarefied Gas Dynamics: 24th International Symposium,* edited by M. Capitelli

Report Documentation Page

Form Approved
OMB No. 0704-0188

1. REPORT DATE	2. REPORT TYPE	3. DATES COVERED
13 JUL 2005	**N/A**	**-**

4. TITLE AND SUBTITLE	5a. CONTRACT NUMBER
Molecular dynamics study on the evaporation part of the kinetic boundary condition at the interface between water and water vapor	5b. GRANT NUMBER
	5c. PROGRAM ELEMENT NUMBER
6. AUTHOR(S)	5d. PROJECT NUMBER
	5e. TASK NUMBER
	5f. WORK UNIT NUMBER
7. PERFORMING ORGANIZATION NAME(S) AND ADDRESS(ES) **Division of Mechanical Science, Hokkaido University, Sapporo 060-8628, Japan**	8. PERFORMING ORGANIZATION REPORT NUMBER
9. SPONSORING/MONITORING AGENCY NAME(S) AND ADDRESS(ES)	10. SPONSOR/MONITOR'S ACRONYM(S)
	11. SPONSOR/MONITOR'S REPORT NUMBER(S)

12. DISTRIBUTION/AVAILABILITY STATEMENT
Approved for public release, distribution unlimited

13. SUPPLEMENTARY NOTES
See also ADM001792, International Symposium on Rarefied Gas Dynamics (24th) Held in Monopoli (Bari), Italy on 10-16 July 2004. , The original document contains color images.

14. ABSTRACT

15. SUBJECT TERMS

16. SECURITY CLASSIFICATION OF:			17. LIMITATION OF ABSTRACT	18. NUMBER OF PAGES	19a. NAME OF RESPONSIBLE PERSON
a. REPORT	b. ABSTRACT	c. THIS PAGE			
unclassified	**unclassified**	**unclassified**	**UU**	**6**	

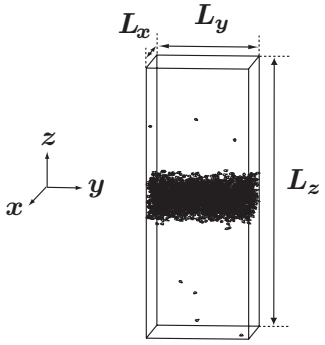

FIGURE 1. Water vapor–water equilibrium in a simulation cell.

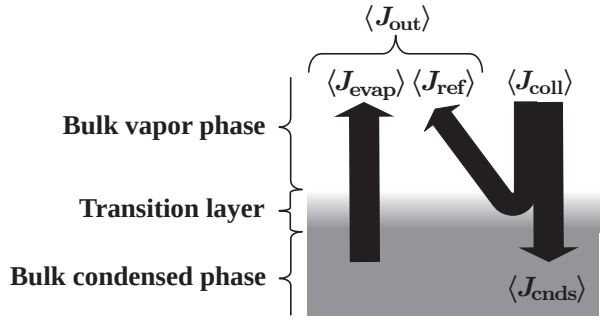

FIGURE 2. Averaged mass fluxes at the vapor-liquid interface.

In this paper, we shall extend the previous study to the case of water. The simulations are carried out in a similar way to the previous one. However, a more careful and detailed analysis is required because a water molecule has the additional degrees of freedom for internal motions and the polarity due to uneven sharing of the bonding electron pair. In particular, the latter induces the formation of molecular clusters in vapor phase and leads to the presence of the preferential orientation of molecules at the interface. Nevertheless, as shown in the present study, we arrive at essentially the same conclusions as the previous study. That is, the distribution function of evaporation can be expressed as

$$\alpha_e \rho_v \hat{f}^* \hat{g}^* \quad (\xi_z > 0), \tag{4}$$

in relatively low temperature cases, where $\rho_v \hat{f}^*$ is the half-Maxwellian for translational motions of center of mass of a polyatomic molecule, which is equal to that given in the right-hand side of Eq. (2) for a monatomic molecule, and $\hat{g}^*$ is the equilibrium distribution associated with internal motions of polyatomic molecule of n degree of freedom,

$$\hat{g}^* = \frac{E^{n/2-1}}{\Gamma(n/2)(kT_\ell)^{n/2}} \exp\left(-\frac{E}{kT_\ell}\right) \quad (0 \le E < \infty), \tag{5}$$

(k is the Boltzmann constant, E is the energy of internal motion of one molecule, and Γ is the gamma function). The symbol $\hat{}$ signifies a normalized distribution function and the superscript $*$ represents that the distribution of molecules is in an equilibrium state.

METHOD OF ANALYSIS

As in the previous study [7], we first define a distribution function of *spontaneous evaporation*, $f_{\rm evap}$, as a distribution function of molecules evaporating from the interface and independent of the condition of incident vapor molecules. This means that $f_{\rm evap}$ is unchanged whether the condensed phase is contact with the vapor or exposed to vacuum and it should be determined by the temperature in the bulk condensed phase only. An arbitrary $f_{\rm out}$ given by MD simulation can then be split into two parts,

$$f_{\rm out} = f_{\rm evap} + f_{\rm ref} \quad (\xi_z > 0), \tag{6}$$

where $f_{\rm ref} = f_{\rm out} - f_{\rm evap}$. Putting $f_{\rm out}$ in the form of Eq. (6) enables us to verify the evaporation part of Eq. (1) in the method explained below. The splitting may also be regarded as the extraction of an inherent property of the bulk condensed phase from $f_{\rm out}$. We shall remark that we don't intend classifying every individual outgoing molecule as either evaporated or reflected one in a vapor–liquid two-phase system; the complete classification may be impossible [6, 7].

Suppose that there are no incoming and reflected molecules at the interface, and then we have from Eq. (6)

$$f_{\rm out} = f_{\rm evap} \quad (\xi_z > 0). \tag{7}$$

Such an extreme situation can be realized in an MD simulation by eliminating vapor molecules at a distance near the interface. We here call this the evaporation into virtual vacuum, or simply, evaporation into vacuum. The functional

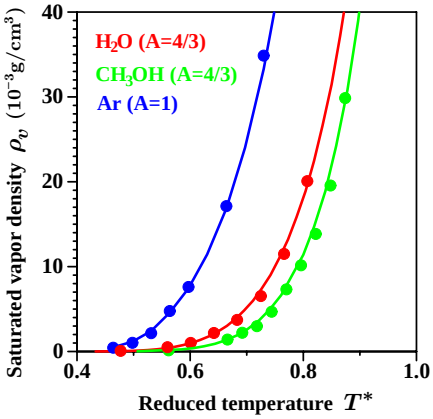

FIGURE 3. Saturated vapor density.

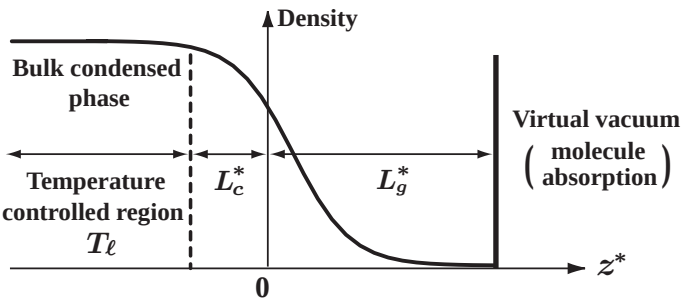

FIGURE 4. Boundary condition and temperature control.

form of f_{evap} can therefore be determined in the MD simulation of evaporation into vacuum by counting the number of evaporating molecules and sampling its velocity.

NUMERICAL METHOD

Intermolecular potential

As an intermolecular potential, we adopt TIP3P model for water [8], since it has been widely used and the computation time is not so large; we have to run many simulations to obtain a large number of samples for the accurate construction of the distribution function. The potential is a 3-site rigid model consist of Lennard–Jones 12-6 potential and Coulomb potential. The additional degree of freedom is $n = 3$ in Eq. (5) and E is the internal energy associated with the rotation of molecule. The intermolecular potential between a site m of a molecule and a site n of a different molecule can be written as

$$\phi_{mn} = 4\varepsilon_{mn}\left[\left(\frac{\sigma_{mn}}{r_{mn}}\right)^{12} - \left(\frac{\sigma_{mn}}{r_{mn}}\right)^{6}\right] + \frac{z_m e_0 z_n e_0}{4\pi\varepsilon_0}\left[\frac{1}{r_{mn}} + \frac{r_{mn}}{r_{\text{cut}}^2} - \frac{2}{r_{\text{cut}}}\right], \tag{8}$$

where r_{mn} is the distance between the site m and the site n, $z_m e_0$ and $z_n e_0$ are partial charges for the sites, e_0 is the elementary charge, ε_0 is the dielectric constant of vacuum, and ε_{mn} and σ_{mn} are the usual Lennard–Jones parameters. As indicated in Eq. (8), the electrostatic term is shifted and scaled smoothly to zero at r_{cut} (0.9 nm), and lattice summation techniques are not used. The applicability of the shifted and scaled Coulomb potential has been confirmed in [9], and it is known that the use of the Ewald summation to the vapor–liquid two-phase system leads to some unnatural behaviors [10]. The Lennard–Jones part also is truncated at the same cutoff distance r_{cut}.

Vapor–liquid equilibrium

In the equilibrium simulations, the periodic boundary conditions are imposed for all three directions of simulation cell. In lower temperature cases of $T_\ell \leq 350$ K, we use the cell of $50 \times 50 \times 200$ Å^3, in which $N = 2000$ molecules are contained, and at higher temperatures $T_\ell \geq 360$ K, we treat 4000 molecules in the longer cell of $50 \times 50 \times 400$ Å. After equilibrating the system, we continue the simulation for 5 ns and accumulate the configurations of all molecules in the cell every 1 ps. Since the system has two interfaces as shown in Fig. 1, the number of samples of configurations is $N_s = 10000$. The ensemble averages for various macroscopic quantities can be evaluated from N_s sampled configurations.

At lower temperatures, the saturated vapor densities calculated with TIP3P model almost agree with experimental values. However, the calculated value of saturated vapor density becomes large compared with experimental one as the

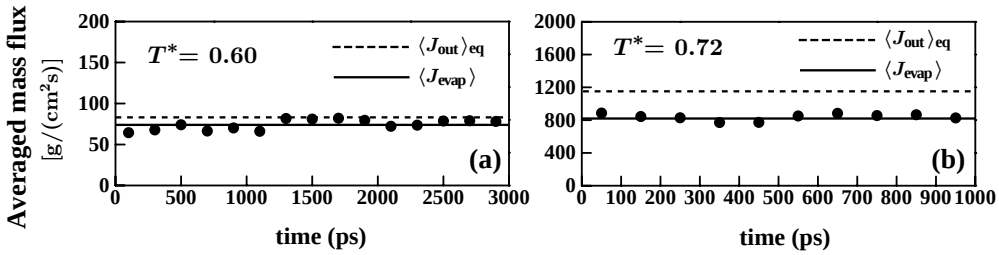

FIGURE 5. Temporal evolution of averaged mass flux. (a): $T^* = 0.60$ ($T_\ell = 340$ K); (b): $T^* = 0.72$ ($T_\ell = 420$ K).

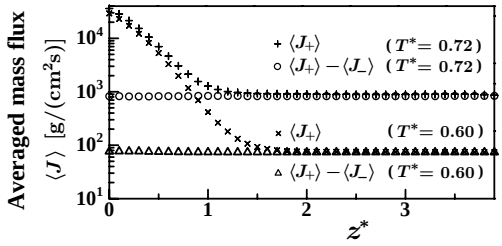

FIGURE 6. Spacial distribution of averaged mass flux.

temperature increases. Therefore, the present results are not directly compared with experimental ones. To compensate the disagreements of saturated vapor density, we arrange the results in terms of a reduced temperature T^* defined by

$$T^* = \frac{T_{\rm triple} + A(T_\ell - T_{\rm triple})}{T_{\rm cr}}, \tag{9}$$

where A is a fitting parameter and $T_{\rm triple}(= 273.2\ {\rm K})$ and $T_{\rm cr}(= 647.1\ {\rm K})$ are experimentally evaluated triple point and critical point temperatures, respectively [11]. As shown in Fig. 3, $A = 4/3$ gives good agreement for water.

Evaporation into virtual vacuum

In the vacuum simulations, we introduce an open boundary at a distance from the interface and eliminate molecules there (Fig. 4), while the periodic boundary conditions are applied in the x and y directions. Molecules evaporate into the virtual vacuum through the open boundary and the interface recedes with time as a result of the evaporation. The steady evaporation state is realized on the moving coordinate

$$z^* = \frac{z - (Z_m - v_s t)}{\delta}, \quad v_s = \frac{J_s}{\rho_\ell}, \tag{10}$$

where δ is the 10-90 thickness of the transition layer whose center is located at Z_m on the original z coordinate, t is the time from the beginning of the vacuum simulation, J_s is a molecular flux evaporating into vacuum, and v_s is the speed of the moving coordinate. The averaged values for macroscopic quantities and the distribution functions are evaluated on the moving coordinate z^*.

The control of the temperature in the bulk liquid phase is essential for the realization of the steady evaporation state. Using the velocity scaling method, we control the temperature of the liquid phase in the region $z^* < -L_c^*$ as shown schematically in Fig. 4. As the result, the averaged temperature of the bulk liquid phase is kept almost uniform and constant at a specified T_ℓ. See Ref. [7] for the detail of the simulation technique.

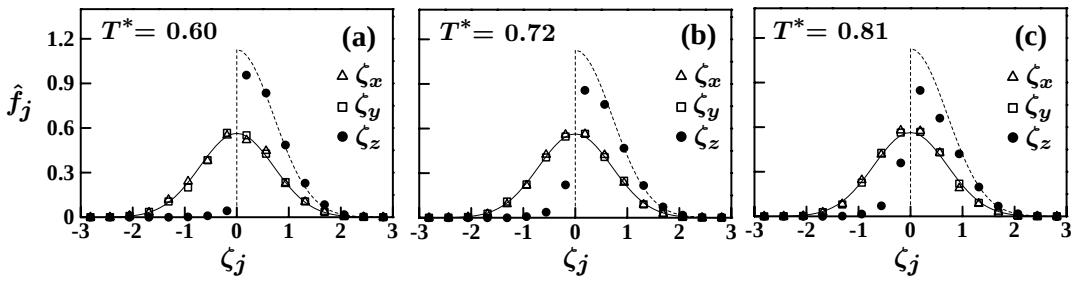

FIGURE 7. Distribution function of translational velocity of the center of mass of molecule.

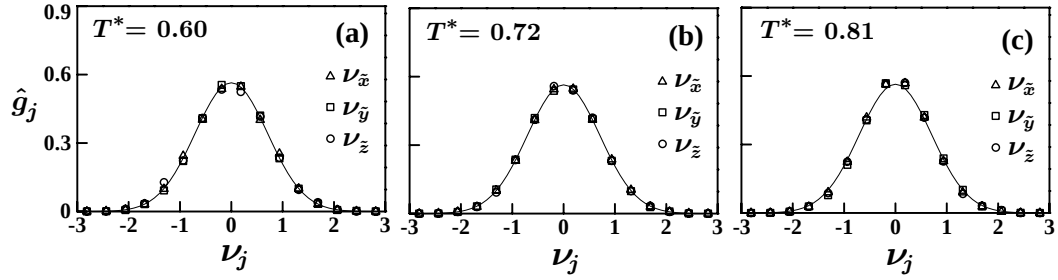

FIGURE 8. Distribution function of angular velocity around the principal axis of water molecule. The principal axes are signified by $\tilde{x}$, $\tilde{y}$, and $\tilde{z}$.

RESULTS AND DISCUSSION

Evaporation mass flux

We shall start with the verification of steadiness of the evaporation into vacuum, because the realization of the steady evaporation state implies the existence of the spontaneous-evaporation mass flux $\langle J_{\rm evap}\rangle$ determined by the bulk liquid temperature T_ℓ only. After an initial transient effect is died out, almost steady evaporation state is established as shown in Fig. 5. The spatial uniformity of the net mass flux is clearly shown in Fig. 6.

Distribution functions

Now, we shall evaluate the distribution function of the translational velocity of molecules evaporating into vacuum, $\hat{f}_{\rm trans}$, and that of internal energy associated with rotational motion, $\hat{g}_{\rm rot}$. In Fig. 7, the velocity distributions of evaporating molecules evaluated at $z^* = L_g^*$ are plotted for some temperatures. The abscissa $\zeta_j = \xi_j/\sqrt{2RT_\ell}$ is the j component of the normalized molecular velocity. Figure 7 shows that the translational velocity distributions of ζ_x and ζ_y denoted by triangles and squares almost agree with a one-dimensional normalized Maxwellian $(1/\sqrt{\pi})\exp(-\zeta_j^2)$ denoted by a solid curve, although those for relatively high T_ℓ cases slightly shift to lower temperature distributions. For relatively low T_ℓ cases shown in Figs. 7(a), the velocity distribution of ζ_z denoted by closed circles becomes nearly a one-dimensional normalized half-Maxwellian $(2/\sqrt{\pi})\exp(-\zeta_j^2)$ $(\zeta_z > 0)$ denoted by a dashed curve.

In Fig. 8, we plot the angular velocity distributions of evaporating molecules at $z^* = L_g^*$. The abscissa $\nu_j = \omega_j\sqrt{I_j/(2kT_\ell)}$ in the figure denotes the normalized angular velocity component around the principal axis. As can be seen from Fig. 8, the angular velocity distributions are isotropic and are nearly the Maxwellians for all temperatures, although the vapor is in an extreme nonequilibrium condition. As in the case of $\hat{f}_{\rm trans}$, $\hat{g}_{\rm rot}$ also slightly shift to lower temperature distributions in higher temperature cases.

Consequently, the distribution function of molecules evaporating into vacuum $f_{\rm evap}$ may be written as the product of ρ_c, $\hat{f}_{\rm trans}$, and $\hat{g}_{\rm rot}$,

$$f_{\rm evap} = \rho_c\,\hat{f}_{\rm trans}\,\hat{g}_{\rm rot} = 2\rho_c\,\hat{f}^*\hat{g}^*, \tag{11}$$

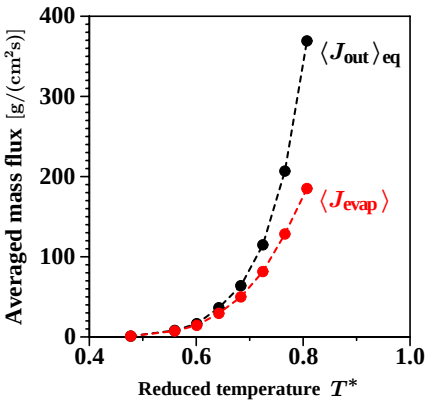

FIGURE 9. Evaporation and outgoing mass fluxes.

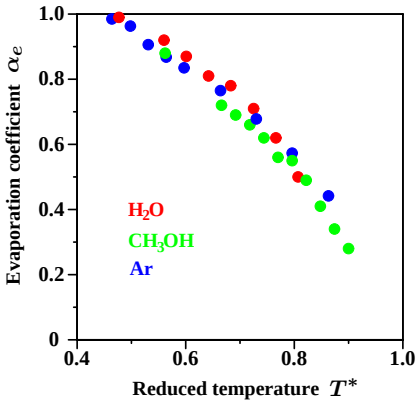

FIGURE 10. Evaporation coefficient.

where ρ_c is the density of the vapor evaporating into vacuum. Using the fact that $\hat{f}_{\text{trans}}$ is the normalized half-Maxwellian, it is easy to show that $\rho_c = \frac{1}{2}\alpha_e \rho_v$ [7], and as a result, we obtain

$$f_{\text{evap}} = \alpha_e \rho_v \hat{f}^* \hat{g}^* = \alpha_e f^{\text{e}}. \tag{12}$$

The evaporation coefficient as a function of T^* is shown in Fig. 10, where the previous results for argon [7] and for methanol [12] are also plotted.

CONCLUSIONS

We have carried out the MD simulations of vapor–liquid equilibrium and those of steady evaporation into the virtual vacuum for water. The distribution function of molecules evaporating into vacuum has been accurately obtained. We have demonstrated that in relatively low temperature case the distribution function is the product of the evaporation coefficient, the half-Maxwellian of translational molecular velocity, and the equilibrium distribution of rotational energy. The evaporation coefficients of water is also determined as a decreasing function of the bulk liquid temperature, and their values are found to become close to unity with decrease in the temperature.

REFERENCES

1. Sone, Y., and Aoki, K., *Molecular Gas Dynamics*, Asakura, Tokyo, 1994, (in Japanese).
2. Cercignani, C., *Rarefied Gas Dynamics*, Cambridge University Press, New York, 2000.
3. Sone, Y., *Kinetic Theory and Fluid Dynamics*, Birkhäuser, Boston, 2002.
4. Tsuruta, T., Tanaka, H., and Masuoka, T., *Int. J. Heat Mass Transf*, **42**, 4107 (1999).
5. Meland, R., and Ytrehus, T., "Boundary condition at a gas-liquid interface," in *Rarefied Gas Dynamics: 22nd International Symposium*, edited by T. J. Bartel and M. A. Gallis, AIP Conference Proceedings 585, American Institute of Physics, New York, 2001, p. 4107.
6. Frezzotti, A., and Gibelli, L., "A kinetic model for equilibrium and non-equilibrium structure of the vapor-liquid interface," in *Rarefied Gas Dynamics: 23nd International Symposium*, edited by A. D. Ketsdever and E. P. Muntz, AIP Conference Proceedings 663, American Institute of Physics, New York, 2003, p. 980.
7. Ishiyama, T., Yano, T., and Fujikawa, S., *Phys. Fluids*, **16**, 2899 (2004).
8. Jorgensen, W. L., Chandrasekhar, J., Madura, J. D., Impey, R. W., and Klein, M. L., *J. Phys. Chem*, **79**, 926 (1983).
9. Kettler, M., Nezbeda, I., Chialve, A. A., and Cummings, P. T., *J. Chem. Phys.*, **106**, 7537 (2002).
10. Mecke, M., and Winkelmann, J., *J. Chem. Phys*, **114**, 5842 (2001).
11. Wagner, W., and Pruss, A., *J. Phys. Chem. Ref. Data*, **31**, 387 (2002).
12. Ishiyama, T., Yano, T., and Fujikawa, S., "Molecular dynamics study of kinetic boundary condition at a vapor-liquid interface for methanol," in *5th International COnference on Multiphase flow, ICMF'04*, 2004.